JOURNAL OF CATALYSIS **161,** 393–400 (1996)
ARTICLE NO. 0197

Initial Activity of Reduced Chromia/Alumina Catalyst in *n*-Butane Dehydrogenation Monitored by On-Line FT–IR Gas Analysis

Arja Hakuli,*,† Arla Kytökivi,† A. Outi I. Krause,* and Tuomo Suntola†

*Helsinki University of Technology, Department of Chemical Engineering, Kemistintie 1, FIN-02150 Espoo, Finland; and †Microchemistry Ltd., P.O. Box 45, FIN-02151 Espoo, Finland

Received June 13, 1995; revised February 9, 1996; accepted February 19, 1996

The initial activity of chromia/alumina catalyst (13 wt% Cr) in *n*-butane dehydrogenation was studied in a flow reactor at 853 K. The initial activity was determined by on-line FT–IR gas analysis, which enabled sampling of the gaseous product mixture at a time resolution of seconds. The catalysts were processed in repeated cycles of oxidation, reduction, and dehydrogenation using *n*-butane, methane, hydrogen, or carbon monoxide as reducing agents. With *n*-butane, methane, and hydrogen the dehydrogenation activity was associated with Cr^{3+} species apparently formed in the reduction of high-valence Cr species. The catalyst reduced with carbon monoxide at 853 K showed poor initial selectivity for butenes and, relative to the other catalysts, stronger formation of coke in dehydrogenation. The initial selectivity for butenes increased with time on stream, however, and within 2 min reached the level obtained with the other catalysts. Simultaneous data relating the initial activity, coke content, and some of the physicochemical properties of the catalyst indicated that the surfaces of all catalysts were modified to some extent by the successive reaction cycles.

INTRODUCTION

Light olefins will be of growing importance in the production of components for reformulated gasoline and city diesel. One way to produce these light olefins is in dehydrogenation processes using catalysts based on chromia. Because of thermodynamic limitations, the dehydrogenation is carried out at elevated temperatures, and the catalyst is rapidly deactivated by coke deposition (1). The combination of the high endothermicity of dehydrogenation and the deactivation of the catalyst represents a particularly difficult challenge for process and catalyst designers. One approach to solving these problems is to run exothermic reactions between moderately short dehydrogenation periods (cyclic reactor operation). The obvious exothermic reaction is burning of the coke. Prereduction of the catalyst can also be included in the operation, since high-valence chromium, inactive in dehydrogenation (2), is produced during the regeneration. In the design of optimal dehydrogenation catalysts and processes, understanding of the origin of the dehydrogenation activity would be of great value.

The characterization of supported chromia catalysts has revealed that Cr may exist on the surface in different oxidation state (6+, 5+, 3+, or 2+) depending on the pretreatment, Cr content, and nature of the support (3, 4). When supported by alumina, chromium mainly occurs in its 3+ oxidation state on a reduced surface (3). Recently, the dehydrogenation activity of chromia/alumina or chromia/zirconia catalysts with 0.04–2.55 wt% Cr has been attributed to coordinatively unsaturated Cr^{3+} species (5–7), although some earlier studies where the Cr content was between 0.1 and 7.3 wt% have suggested the activity of Cr^{2+} species as well (8–11). According to De Rossi *et al.* (5), prereduction of the chromia/alumina catalyst with carbon monoxide or hydrogen before propane dehydrogenation does not influence the activity. In a study of the aromatization activity of prereduced chromia/alumina catalysts (10.5 wt% Cr), Grünert *et al.* (12) likewise found that the nature of the reducing agent (H_2, CH_4, *n*-C_6H_{14}, or CO) did not influence the activity. Gorriz *et al.* (2) nevertheless found slight differences in the dehydrogenation activity depending on the reducing agent (H_2, C_3H_8, or CO). Following the reaction for several hours, while determining the product distribution with a gas chromatograph, they suggested that the main differences occured during the first 10 min on stream.

Since there is no general agreement about the effect of reducing agent on the initial activity, the subject was studied further in this work using a FT–IR gas analyzer. Unlike gas chromatography, the FT–IR technique allowed us to continuously monitor the very first stages of the reaction and it thus provided a suitable way of studying the initial dehydrogenation activity on a prereduced surface. The catalysts were processed in repeated cycles of oxidation, reduction, and dehydrogenation using *n*-butane, methane, hydrogen, or carbon monoxide as reducing agents. The origin of the dehydrogenation activity is discussed in light of the initial activity and some physicochemical properties of the catalyst.

0021-9517/96 $18.00

EXPERIMENTAL

Catalyst Preparation and Characterization

A γ-alumina layer (36 μm) carried by a metallic sheet of cylindrical shape was used as support for the chromia catalysts (13, 14). The weight of the alumina layer corresponded to 26 wt% of the weight of the sheet. After heating at 1027 K in air for 2 h, the alumina was impregnated with an aqueous solution of $Cr(NO_3)_3 \cdot 9H_2O$. Before use, the samples were dried at 400 K for 1 h and calcined in air at 873 K for 16 h. The alumina layer contained 13 wt% chromium (instrumental neutron-activation analysis, INAA), corresponding to the chromium content of commercial chromia/alumina catalysts (15). The calcined catalysts contained Cr_2O_3 crystallites (Siemens Diffrac 500/X-ray source Cu$K\alpha$). The surface areas of the fresh and used catalysts were determined by nitrogen adsorption and condensation (Micromeritics ASAP 2400). The catalysts were not separated from the metallic sheet for the analysis of BET areas and thus the reported BET areas are quite low. The specific BET area of alumina separated from the metallic sheet was 160 m^2/g.

X-ray photoelectron spectra of the catalysts were recorded with a Surface Science Instruments (S.S.I./Fisons) X-probe model 101 spectrometer. The spectrometer was equipped with a monochromatized Al$K\alpha$ X-ray source. The catalyst samples for XPS analysis were reduced in the test reactor and were inertly transferred to the glove box of the spectrometer in a closed reactor tube. Reduction of Cr^{6+} by impinging X rays during XPS analysis was minimized by using a short analysis time. The curve fitting of Cr $2p_{3/2}$ spectra was accomplished with a standard peak synthesis program. The Al $2p$ line of the alumina support assumed to be at 74.5 eV was used as an internal binding energy reference for the samples. The following assumptions were introduced into the curve fitting: (i) the distance and the intensity ratio between the Cr $2p_{3/2}$ main and satellite lines for Cr^{3+} species are 4.1 eV and 3.125, respectively (16), (ii) only Cr^{3+} has a satellite line, (iii) peaks are symmetric Gaussian, and (iv) the background is nonlinear Shirley. The relative surface composition in atomic percent was calculated from the spectra for chromium (Cr $2p_{3/2}$), aluminum (Al $2p$), and oxygen (O $1s$) using atomic sensitivity factors provided by the instrument manufacturer.

The quantitative analysis of the catalysts for Cr^{6+} species was performed with a UV-VIS spectrophotometer. The analysis was carried out by dissolving Cr^{6+} species from the catalysts and by determining Cr^{6+} as chromate in alkaline solution at 372 nm. The method is described in detail elsewhere (17).

Test Reactor and FT–IR Gas Analyzer

The reactor setup consisted of an automated laboratory-scale flow reactor and an on-line FT–IR gas analyzer with a program for the analysis of IR spectra (Gasmet, Temet Instruments Ltd.). The FT–IR gas analyzer covered the range 1000–4000 cm^{-1}, with a resolution of 8 cm^{-1} and a scanning rate of 12 scans/s. The temperature and pressure of the continuous flow IR cuvette (9 cm^3) were maintained constant at 448 K and 101 kPa, respectively, to ensure reliable gas-phase analysis. The analyzer was calibrated with *n*-butane, 1-butene, *cis*-2-butene, *trans*-2-butene, i-butane, i-butene, 1,3-butadiene, propane, propene, ethane, ethene, methane, toluene, benzene, carbon dioxide, carbon monoxide, and water vapor. The purity of the calibration gases was better than 99%, except for propane (98%) and *cis*-2-butene (95%).

The measured IR spectra were interpreted by the method of Saarinen and Kauppinen (18), which was earlier tested in the analysis of a reference gas mixture of hydrocarbons typically produced in the dehydrogenation of *n*-butane (19). In this method, the partial pressures of the gases in the sample are determined by searching for the linear combination of calibration spectra best explaining the measured sample spectrum. All wavenumbers at which the absorbance in the sample spectrum was smaller than 0.6 were used in the fits. The quality of the fit was checked from the residual spectrum obtained by subtracting the fitted from the measured spectrum. Ideally, the residual spectrum is pure noise. An example of a sample spectrum of the dehydrogenation product mixture and the corresponding residual spectrum is presented in Fig. 1. All the calibrated hydrocarbons were

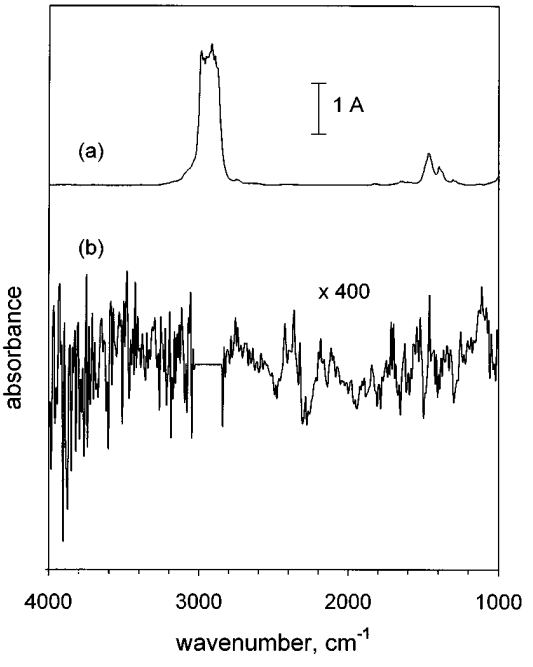

FIG. 1. Spectrum obtained (a) from the dehydrogenation product mixture and (b) by subtracting the measured spectrum from the set of calibration spectra. Wavenumbers at which absorbance exceeded 0.6 were excluded from the analysis.

detected in the product mixtures. When the number of carbon atoms from coke were considered, a value close to 100% was obtained for carbon mass balance. This indicates that no significant amounts of other carbon-containing compounds were produced.

Experimental Procedure

Catalyst samples of 0.26 g (weight of the metallic carrier excluded) were used in the activity measurements. First, the calcined catalysts were aged in 10 consecutive dehydrogenation–oxidation cycles (reference cycles) at 853 K. The dehydrogenation feed gas consisted of *n*-butane diluted with nitrogen (50 vol%), with a total gas flow of 82 cm^3/min (STP). The oxidation gas was 5 vol% oxygen diluted with nitrogen with a gas flow of 330 cm^3/min (STP). The dehydrogenation and oxidation periods were 2 and 40 min, respectively. After 10 reference cycles the reduction of the catalyst with methane, hydrogen, or carbon monoxide at 853 K was included in the procedure, and the catalysts were subjected to 15 or 16 reduction–dehydrogenation–oxidation cycles. With carbon monoxide the reduction was also performed at 673 K. The reduction periods were 4 or 20 min using a total flow rate of 330 cm^3/min (STP) of CO, CH_4, or H_2 diluted with nitrogen (10 vol%). The stability of the catalyst activity during the cycling was probed by performing some reference cycles in between. In some runs, the dehydrogenation was omitted and the reduced catalyst was oxidized directly. From these reduction–oxidation cycles, the amount of carbon or hydrogen retained in the catalyst solely from the reducing agent was determined.

The product mixtures were sampled for 0.08–2 s at time intervals of 1–8 s depending on the case. The measurement time was 2 s if water was among the detected products; water has low absorptivity and a longer measurement time was required to obtain signal-to-noise ratios high enough in the spectra.

RESULTS

Catalyst Activity and Stability in Consecutive Reference Cycles

An example of the product distribution obtained in the dehydrogenation of *n*-butane on unreduced catalyst is presented in Fig. 2. The reduction of the high-valence chromium species with *n*-butane at the beginning of the dehydrogenation was seen as a release of carbon dioxide. Carbon monoxide was released as well, but in a smaller amount. In agreement with the results of Grünert *et al.* (12), a release of water commensurate with the amount of carbon released (as CO_2 and CO) was not detected, even though water was expected to be formed in the oxidation of *n*-butane.

After the reduction of the catalyst with *n*-butane, the product distribution remained nearly constant during the

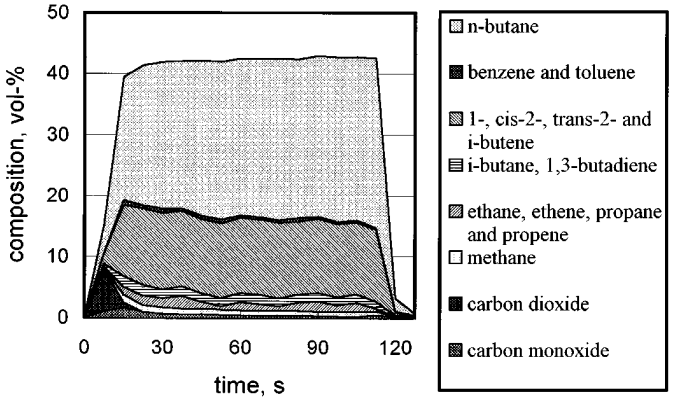

FIG. 2. The product distribution of reference dehydrogenation cycle monitored with an FT-IR gas analyser using a measurement time of 1 s (feed: *n*-butane/nitrogen = 1 : 1 (mol/mol), $T = 853$ K).

2-min dehydrogenation period. From this period of "constant" activity, a mean conversion and selectivity for butenes (1-, *cis*-2-, *trans*-2-, and i-butene) was calculated, to allow the activity of the catalyst to be followed in subsequent reference cycles (Fig. 3). The catalyst lost about 25% of its original activity during the reference cycles. At the same time the selectivity for butenes increased slightly. Although the data in Fig. 3 refer to the catalyst used in the hydrogen reductions, they equally well describe the behavior observed with the catalysts used in carbon monoxide

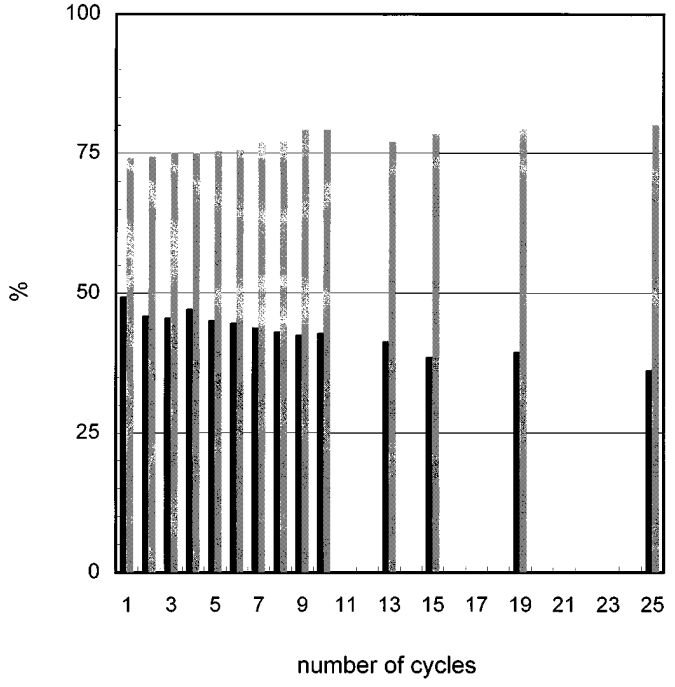

FIG. 3. The conversion (black bars) and selectivity (gray bars) of chromia/alumina in successive reference dehydrogenation cycles. Cycles 11–12, 14, 16–18, and 20–24 included prereduction of the catalyst.

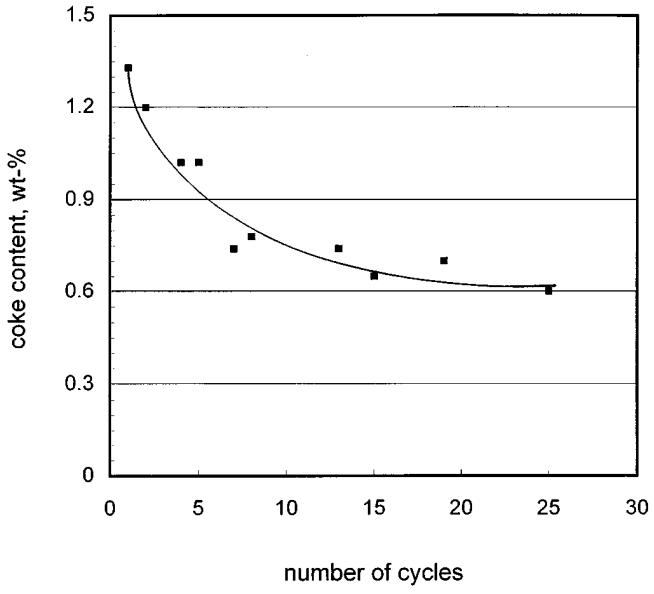

FIG. 4. The amount of coke deposited on the catalyst in successive reference dehydrogenation cycles at 853 K.

and methane reductions. During the first 10 reference cycles, the decay of the initial activity of the catalyst was accompanied by a significant decrease in the amount of coke deposited. The coke deposition then leveled off at a constant level of about 0.65 wt% (Fig. 4).

The cycling of the catalyst under oxidizing and reducing conditions also affected its physicochemical properties. The specific BET surface area of the used catalyst (24 m^2/g) was about 14% less than the specific BET surface area of the fresh calcined catalyst (28 m^2/g). In addition, the ratio of the intensities of the crystalline chromia and alumina peaks was higher in the used catalysts. The average size of chromia crystallites in the samples was 40–50 Å (from the Scherrer equation) and the size did not change during the cycling. The UV-VIS measurements showed the amount of Cr^{6+} as determined in the oxidized catalyst to decrease with the number of cycles (Table 1). In the calcined catalyst 15% of the chromium was in the oxidation state 6+, whereas after 25–26 cycles, the amount was 12.7 ± 0.3%. Thus, part of the Cr^{6+} was irreversibly reduced to a lower oxidation state in successive reaction cycles. The UV-VIS results were supported by the temperature measurements in the reactor: The temperature increase at the beginning of the reference dehydrogenation cycle became smaller as the number of cycles increased, since less Cr^{6+} was reduced to lower valence with *n*-butane ($\Delta H_{red.} < 0$; $\Delta H_{dehydr.} > 0$).

TABLE 1

Amount of Cr^{6+} Determined in Oxidized Chromia/Alumina Catalysts by UV-VIS Spectroscopy

Treatment	Cr^{6+}(wt%)
Calcined	1.99
Cycled/10 Ref.[a]	1.85
Cycled/CH_4[b]	1.67
Cycled/H_2[b]	1.67
Cycled/CO[b]	1.61

[a] Calcined catalyst used in 10 reference cycles.
[b] Catalyst used in 10 reference cycles and in 15–16 reaction cycles that included the prereduction.

The Effect of Prereduction of the Catalyst on Activity

The conversion and selectivity for butenes of the catalysts prereduced with methane, hydrogen, and carbon monoxide are presented in Fig. 5. The prereduction of the catalyst with methane did not influence the activity or the selectivity. The effect of hydrogen prereduction was hardly noticeable, since only a slightly lower initial activity and a slightly higher initial selectivity were obtained. Distinct and clearly different results were obtained with the catalyst reduced with carbon monoxide: The formation of cracking products (C_1–C_3) was increased during the first 60 s on stream and the initial selectivity for butenes was low. However, the selectivity for butenes increased with the reaction time and within 2 min reached 80%, which was the selectivity obtained with methane-, hydrogen-, and *n*-butane-reduced catalysts. The effect of the carbon monoxide prereduction depended on the reduction temperature; the prereduction of the catalyst at 673 K did not affect the activity or the selectivity. The prereduction time (4–20 min)

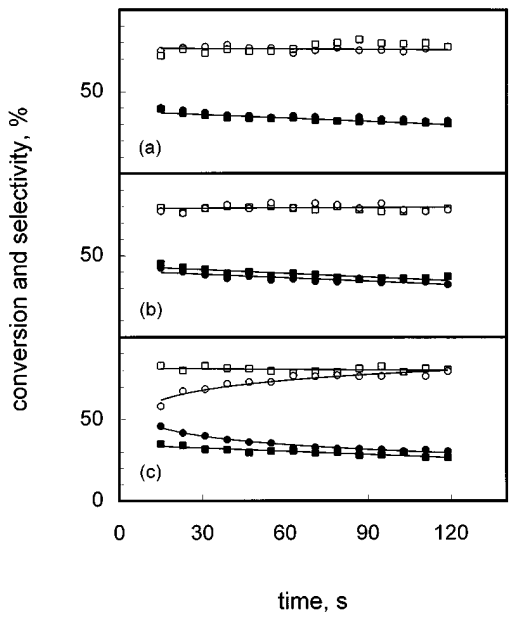

FIG. 5. The activity of the catalyst prereduced with (a) methane, (b) hydrogen, or (c) carbon monoxide in *n*-butane dehydrogenation at 853 K. Conversion (●) and selectivity (○) on prereduced catalyst (CH_4/H_2/CO); conversion (■) and selectivity (□) on catalyst reduced with *n*-C_4H_{10}.

did not affect the initial activity or selectivity and Fig. 5 represents the results after 4-min reductions.

The observed differences in the initial activities were reflected in the amounts of coke deposited on the catalysts during the dehydrogenation. The total coke content of the catalyst prereduced with carbon monoxide at 853 K was the highest, at 2.0 ± 0.2 wt%. If the prereduction with carbon monoxide was performed at the lower reduction temperature of 673 K, the coke content was at the same level as with the catalysts reduced with methane or *n*-butane (0.65 ± 0.1 wt%). The hydrogen prereduction of the catalyst seemed to slightly inhibit the coke formation, the coke content being 0.50 ± 0.1 wt%.

Catalyst Prereduction

The differences observed in the initial activities of catalysts led us to determine the valences of the reduced chromium species. With the FT–IR gas analyzer, the extent of the reduction with methane, hydrogen, and carbon monoxide was estimated on the basis of the amount of oxygen released in the reduction products (CO_2, H_2O). We assumed in the calculation that initially all the reducible chromium was in oxidation state 6+. This being the case, 1 and 2 mol of atomic oxygen released per mol of Cr^{6+} would indicate reduction to chromium 4+ and chromium 2+, respectively.

Methane. Carbon dioxide was the only product detected in methane reductions. No water was detected, but it was released during the subsequent oxidation. The molar amount of hydrogen released as H_2O during the oxidation was 3.8 times the amount of carbon dioxide released in the reduction (0.5 ± 0.1 mol CO_2/mol Cr^{6+}). This molar ratio of hydrogen and carbon is close to the H/C ratio of methane, suggesting that the hydrogen initially bonded in methane was retained in the catalyst during the reduction. In addition, a small amount of carbon from methane was retained in the catalyst as indicated by the carbon dioxide released during the subsequent oxidation (0.08 ± 0.02 mol CO_2/mol Cr^{6+}). The retainment of hydrogen and a small amount of carbon in the catalyst is in agreement with previous findings (12). Because of the retainment of hydrogen in the catalyst, the amount of oxygen released during the reduction does not reveal the true extent of reduction. Accordingly, an average oxidation state higher than 3+ was obtained. The total amount of carbon dioxide and water released corresponded, however, to a reduction to the 3+ oxidation state.

Hydrogen. The reduction of the catalyst with hydrogen was seen as a release of water. In successive cycles, the amount of water released decreased slightly but detectably in parallel with Cr^{6+}. As in the reductions with methane, part of the hydrogen from the reducing agent was retained in the catalyst. In agreement with De Rossi *et al.* (6) and Grünert *et al.* (12), we found the amount of water released during the reduction to be equal to the amount of water released during the subsequent oxidation, viz. 0.7 ± 0.2 mol H_2O/mol Cr^{6+}. The amount of water released during the oxidation did not depend on the duration of the nitrogen flush (5–20 min) between the reduction and oxidation. The amount of oxygen released during the reduction and the subsequent oxidation corresponded to an average oxidation state of 3+.

Carbon monoxide. The amount of oxygen released as carbon dioxide during the reduction with carbon mono xide decreased slightly but detectably in successive cycles. A similar trend was observed with hydrogen, while with methane the decrease was not so clear. Judging from the amount of oxygen released, the reduced chromium was in oxidation state 3+ (1.5 ± 0.2 mol/mol Cr^{6+}). As in the reductions with methane, part of the carbon (0.1 ± 0.01 mol C/mol Cr^{6+}) was retained in the catalyst during the reduction and was detected as a release of carbon dioxide when the catalyst was exposed to oxygen. Reduction at the lower temperature of 673 K indicated a lower extent of reduction, and the amount of carbon dioxide released corresponded to oxidation state 4+ (1.1 ± 0.02 mol/mol Cr^{6+}).

XPS Measurements

To obtain supplementary information about the reductions, the extent of the reductions was determined by XPS. Measurements were carried out on calcined, reduced, and cycled samples (Table 2). The curve fitting for the Cr $2p_{3/2}$ line showed the presence of Cr^{3+} and Cr^{6+} in the samples,

TABLE 2

Binding Energies (E_b), Extent of Reduction (Cr^{6+}/Cr^{3+}), and Atomic Ratio between Cr and Al (Cr/Al) in Calcined, Reduced ($CH_4/H_2/CO$), Reoxidized, and Cycled Samples[a]

Catalyst	E_b (Cr^{3+}) (eV)	E_b (Cr^{6+}) (eV)	Cr^{6+}/Cr^{3+} [b]	Cr/Al
Calcined	576.9	579.8	0.35	0.17 ± 0.01
Reduced; CH_4	577.1	579.6	<0.10	0.13
Reoxidized	576.9	579.6	0.40	0.15
Cycled/oxidized[c]	577.0	579.4	0.15	0.17
Reduced; H_2	577.0	579.5	<0.10	0.12
Reoxidized	577.1	579.6	0.40	0.14
Cycled/oxidized[c]	577.0	579.3	0.15	0.15
Reduced; CO	577.0	579.5	<0.10	0.12
Reoxidized	576.7	579.6	0.30	0.19
Cycled/oxidized[c]	576.9	579.3	0.20	0.18

[a] The Al 2*p* line of the support (74.5 eV) was used as an internal BE reference for the samples. The atomic ratio between Cr and Al was calculated from Cr $2p_{3/2}$ and Al 2*p* lines.

[b] The actual values for Cr^{6+}/Cr^{3+} are higher than indicated in the table, since photoreduction of Cr^{6+} was unavoidable during the measurement.

[c] Oxidized catalyst used in 10 reference cycles and in 15–16 reaction cycles that included the prereduction.

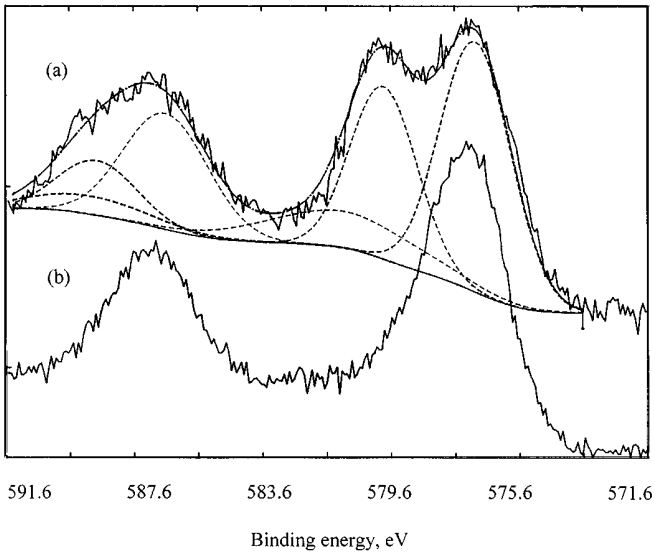

FIG. 6. XPS spectrum of the Cr 2*p* region recorded from (a) calcined catalyst (curve fitting with Cr^{6+}, Cr^{3+}, and satellite of Cr^{3+} inserted) and (b) reduced catalyst.

at 576.7–577.1 eV and 579.3–579.8 eV, respectively (Fig. 6). These binding energies are close to the binding energies of 577.3 eV (Cr^{3+}) and 579.9 eV (Cr^{6+}) reported by Grünert *et al.* (16). Independent of the reducing agent, more than 90% of the high-valence chromium was reduced to 3+ during the 4-min reduction. No evidence of the presence of oxidation states other than Cr^{3+} and Cr^{6+} was found on either the reduced or oxidized surface.

When reduction was at 853 K, the XPS results regarding the extent of the reductions were consistent with the results obtained with the FT–IR gas analyzer, provided that in the reductions with methane and hydrogen the amount of water released during the subsequent oxidation was included. After reduction with carbon monoxide at 673 K, the XPS suggested a higher extent of reduction than the FT–IR gas analyzer. Perhaps this was due to slightly different sample handling. In the reactor, part of the oxidized 6+ species might have been reduced when the catalyst was cooled from 853 K to the reduction temperature of 673 K. During the cooling the catalyst was kept under a nitrogen flow, in which the 6+ species might not be as stable as in oxygen (20) and consequently a lower amount of carbon dioxide would be released. The samples used in the XPS measurements were oxidized at 673 K prior to the reduction.

In addition to determining the oxidation states of chromium, we also used XPS to measure the atomic ratios of the chromium and aluminum in the calcined, reduced, reoxidized, and cycled samples (Table 2). The reduction of the catalyst with methane, hydrogen, or carbon monoxide produced a decrease in the chromium-to-aluminum concentration ratio. In the oxidized samples, even though these were used in several reaction cycles, the chromium-to-aluminum concentration ratio was restored. In XPS, a decrease in the metal-to-support signal ratio indicates a decrease in dispersion, provided that the distribution of chromium in alumina particles remained unchanged.

DISCUSSION

The Active Oxidation State of Chromium

The hydrogen precovered surface obtained in methane, hydrogen, and *n*-butane reductions was more favorable for the dehydrogenation reaction than the "hydrogen-free" catalyst surface resulting from the carbon monoxide reduction at 853 K. The catalyst reduced with carbon monoxide at 853 K showed higher initial selectivity for cracking products and a pronounced deposition of carbonaceous material, characteristic of catalytic cracking. However, when the reduction with carbon monoxide was performed at 673 K, activity similar to that after reductions with *n*-butane, methane, and hydrogen was observed. Hence, the cracking activity of the surface reduced with carbon monoxide at 853 K could not be explained by the absence of the "retained hydrogen" from the surface but could indicate different oxidation state of chromium depending on the reducing agent.

The water–gas equilibrium ($CO+H_2O \rightleftharpoons H_2+CO_2$) and experimental results (5, 21) suggest carbon monoxide to be a slightly more powerful reducing agent than hydrogen. Accordingly, the cracking activity might have been due to the presence of chromium in a lower oxidation state after carbon monoxide reduction at 853 K than after reductions with hydrogen, methane, or *n*-butane at 853 K or with carbon monoxide at 673 K. This proposal is supported by the measurements of Niemi (22), who has shown silica-supported chromia, which is easily reduced to 2+ (23, 24), to possess a high selectivity for cracking products in *n*-butane dehydrogenation. Although our experimental results do not provide evidence for the existence of Cr^{2+} in the carbon monoxide-reduced catalyst, we would note the difficulty of detecting Cr^{2+} by XPS, especially if the Cr^{2+} is present in a small amount (25). In fact, although its presence on alumina carrier has been confirmed by IR and DRS studies in samples with 0.07–4.8 wt% Cr (26, 27, 3), to our knowledge it has never been detected by XPS.

Characteristic to the dehydrogenation activity on catalyst reduced with carbon monoxide at 853 K was that the cracking activity decayed quite rapidly. Within 60 s the catalyst lost its cracking activity and became increasingly active in dehydrogenation. The surface sites formed in the reduction with carbon monoxide probably evolved to the same type of sites formed in the methane, hydrogen, or *n*-butane reductions. The findings of De Rossi *et al.* (5), particularly the instability of Cr^{2+} in the presence of propane, support our assumption that Cr^{2+} species were present on the surface after prereduction with carbon monoxide. Hence, the decaying

of the cracking activity in the *n*-butane stream might have been due to the transformation of Cr^{2+} to Cr^{3+}, which is assumed to be the active site in dehydrogenation. Probably, the use of gas chromatography in the analysis of the product mixtures prevented De Rossi *et al.* (5) from observing the differences in the initial activities between catalysts reduced with carbon monoxide and with hydrogen; we note, however, that they found a higher extent of reduction after carbon monoxide than after hydrogen treatment in IR measurements of adsorbed probe molecules (CO/NO).

Deactivation of the Catalyst

The aging of the catalyst in repeated cycles was seen as decreased initial activity and decreased formation of coke. In addition, the amount of Cr^{6+} determined in the oxidized catalyst decreased with the number of cycles. In agreement with Masson *et al.* (7), we suggest that the high-valence chromium species were precursors of the active sites of the catalyst, since the amount of Cr^{6+} decreased parallel to the initial activity (Fig. 7). The suggestion is supported by the observed influence of the reducing agent on the selectivity. If these high-valence species had nothing to do with the active species of the catalyst, the reducing agent should not have had the influence it did on the selectivity. Thus, the deactivation of the catalyst in successive cycles was probably due to the decreasing number of active sites available on the surface. It is noteworthy that the chemical quantitation of Cr^{6+} species might also have included Cr^{5+} species if these were present on the surface. We underline, therefore, that our results do not exclude the possibility that active Cr^{3+} species could arise from reduction of Cr^{5+} species. Indeed, based on ESR measurements, De Rossi *et al.* (5, 6) have concluded that Cr^{5+} species are the precursors of the active Cr^{3+}.

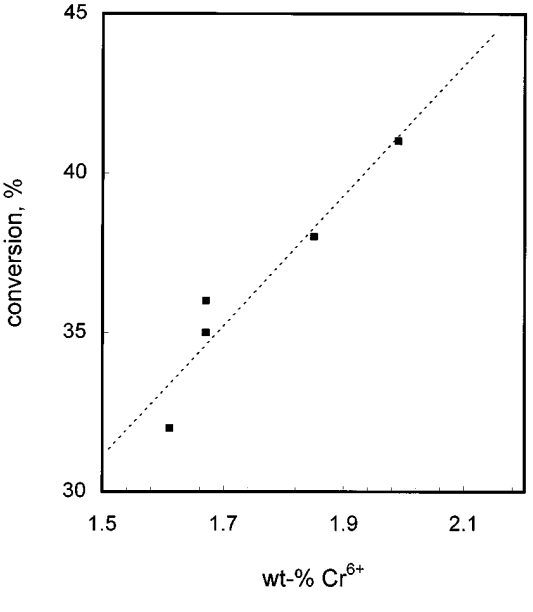

FIG. 7. The correlation between activity and the amount of Cr^{6+} as determined in the calcined and used catalysts.

It seems that those Cr^{3+} species that could not be oxidized to higher oxidation state were inactive in the dehydrogenation reaction for the following reasons. First, many of these Cr^{3+} atoms belonged to the bulk chromia phase and were therefore not surface atoms. Second, there is evidence in the literature that isolated Cr^{3+} species that resist oxidation are stabilized in or on alumina (28). It is reasonable to assume that these species, in strong interaction with alumina, would not be active even if they were present on the surface. The formation of Cr^{3+} species from the higher-valence states, on the other hand, would give rise on the surface to coordinatively unsaturated chromium species (6).

Judging from the stabilizing effect of alumina on Cr^{6+} (29), the decrease in the Cr^{6+} content with the aging of the catalyst was related to the rearrangement of chromium on the surface. The decrease of the surface area may be one reason for the rearrangement. Other factors leading to disappearance of Cr^{6+} sites may have been agglomeration of chromium on the surface or diffusion of chromium species into the alumina support. In both cases inactive material that is not easily oxidized is formed (3). The XRD measurements confirmed the formation of chromia crystallites on the surface during the processing. This is in agreement with the literature, where the agglomeration of chromium at elevated temperatures and especially in the presence of water is widely reported (21, 24, 30, 31). The XPS results did not reveal the agglomeration of chromium during the cycling, but instead suggested a rearrangement of chromium on the surface in the shorter term: The Cr-to-Al atomic ratio decreased considerably after one reduction treatment but was then restored in the subsequent oxidation. Whether this is related to changes in the dispersion of chromium induced by pretreatment or to some other phenomena is not, so far, established. In the literature, there is evidence for the formation of chromia aggregates under reducing conditions and the redispersion of these aggregates by oxidation (29, 32, 33). It is surprising, however, that the overall decrease in the dispersion of chromium during aging, as suggested by UV-VIS analysis of Cr^{6+} and XRD measurements, was not detectable with XPS.

CONCLUSIONS

The multicomponent analysis of IR spectra allowed us to exploit the rapidity of the FT–IR method in a study of the initial activity of chromia/alumina catalyst. Besides the initial activity, the coke content and the extent of the reduction of the catalyst with carbon monoxide, methane, hydrogen, and *n*-butane were monitored *in situ*. The catalyst reduced with carbon monoxide at 853 K showed poor initial selectivity for butenes and, relative to the other catalysts, stronger formation of coke. However, the selectivity for butenes

increased with the time on *n*-butane stream, and within 2 min reached the level obtained with *n*-butane, methane, and hydrogen-reduced catalysts. This initial cracking activity was attributed to a deeper reduction of chromium with carbon monoxide at 853 K than with *n*-butane, methane, or hydrogen. The surface of all the catalysts was modified to some extent in successive oxidation–reduction–dehydrogenation cycles, as seen in the decreasing amount of Cr^{6+} in the oxidized catalyst. Furthermore, the initial dehydrogenation activity and the amount of coke that was deposited decreased with the number of reaction cycles. On the basis of the initial activity and the XPS and UV-VIS measurements, the dehydrogenation activity was associated to Cr^{3+} species perhaps formed in the reduction of high-valence chromium species.

ACKNOWLEDGMENTS

This work was supported by the Academy of Finland and Ministry of Education of Finland. We are grateful to Kemira Metalcat Ltd. for preparing the catalysts and to O. Jylhä, I. Savolainen, M. Rissanen, and the Scientific Services of Neste Co. for characterizing the catalysts. We acknowledge with thanks the valuable comments of Tech. Lic. Vesa Niemi from Corporate R&D Neste Co.

REFERENCES

1. Dumez, F. J., and Froment, G. F., *Ind. Eng. Chem. Process Des. Dev.* **15**, 291 (1976).
2. Gorriz, O. F., Cortés Corbéran, V., and Fierro, J. L. G., *Ind. Eng. Chem. Res.* **31**, 2670 (1992).
3. Weckhuysen, B. M., De Ridder, L. M., and Schoonheydt, R. A., *J. Phys. Chem.* **97**, 4756 (1993).
4. Okamoto, Y., Fujh, M., Imanaka, T., and Teranishi, S., *Bull. Chem. Soc. Jpn.* **49**, 859 (1976).
5. De Rossi, S., Ferraris, G., Fremiotti, S., Garrone, E., Ghiotti, G., Campa, M. C., and Indovina, V., *J. Catal.* **148**, 36 (1994).
6. De Rossi, S., Ferraris, G., Fremiotti, S., Indovina, V., and Cimino, A., *Appl. Catal.* **106**, 125 (1993).
7. Masson, J., Bonnier, J. M., Duvigneaud, P. H., and Delmon, B., *J. Chem. Soc. Faraday Trans. 1* **73**, 1471 (1977).
8. Ashmawy, F. M., *J. Chem. Soc. Faraday Trans. 1* **76**, 2096 (1980).
9. Lugo, H. J., and Lunsford, J. H., *J. Catal.* **91**, 155 (1985).
10. Sterligov, O. D., Gitis, K. M., Slovetskaya, K. I., Shapiro, E. S., Rubinstein, A. M., and Minachev, K. M., *in* "Catalyst Deactivation 1980" (B. Delmon and G. F. Froment, Eds.), Proc. 2nd Int. Symp. Catal. Deact., p. 363. Elsevier, Amsterdam, 1980.
11. Marcilly, Ch., and Delmon, B., *J. Catal.* **24**, 336 (1972).
12. Grünert, W., Saffert, W., Feldhaus, R., and Anders, K., *J. Catal.* **99**, 149 (1986).
13. Luoma, M., Torkkell, K., Lylykangas, R., and Virta, P., Patent WO 92/11936.
14. Härkönen, M., Ravola, S., and Kivioja, M., Patent WO 93/22051.
15. Craig, R. G., and Duffallo, J. M., *Chem. Eng. Prog.* **75**, 62 (1979).
16. Grünert, W., Shpiro, E. S., Feldhaus, R., Anders, K., Antoshin, G. V., and Minachev, Kh. M., *J. Catal.* **100**, 138 (1986).
17. Haukka, S., *Analyst* **116**, 1055 (1991).
18. Saarinen, P., and Kauppinen, J., *Appl. Spectrosc.* **45**, 953 (1991).
19. Hakuli, A., Kytökivi, A., Lakomaa, E.-L., and Krause, O., *Anal. Chem.* **67**, 1881 (1995).
20. McDaniel, M. P., *J. Catal.* **76**, 37 (1982).
21. Groeneveld, C., Wittgen, P. P. M. M., van Kersbergen, A. M., Mestrom, P. L. M., Nuijten, C. E., and Schuit, G. C. A., *J. Catal.* **59**, 153 (1979).
22. Niemi, V. M., unpublished results.
23. Weckhuysen, B. M., Verberckmoes, A. A., Buttiens, A. L., and Schoonheydt, R. A., *J. Phys. Chem.* **98**, 579 (1994).
24. Zecchina, A., Garrone, E., Ghiotti, G., Morterra, C., and Borello, E., *J. Phys. Chem.* **79**, 966 (1975).
25. Scierca, S. J., Proctor, A., Houalla, M., Fiedor, J. N., and Hercules, D. M., *Surf. Interface Anal.* **20**, 901 (1993).
26. Peri, J. B., *J. Phys. Chem.* **78**, 588 (1974).
27. Rebenstorf, B., and Andersson, S. L. T., *J. Chem. Soc. Faraday Trans. 1* **86**, 3153 (1990).
28. Weckhuysen, B. M, De Ridder, L. M., Grobet, P. J., and Schoonheydt, R. A., *J. Phys. Chem.* **99**, 320 (1995).
29. Ellison, A., and Sing, K. S. W., *J. Chem. Soc. Faraday Trans. 1* **74**, 2017 (1978).
30. Welch, M. B., and McDaniel, M. P., *J. Catal.* **82**, 110 (1983).
31. Peña, J. A., Monzón, A., Santamaría, J., and Fierro, J. L. G., *Appl. Catal.* **101**, 185 (1993).
32. Jozwiak, W. K., Dalla Lana, I. G., Paryjczak, T., "Europacat-I, Book of Abstracts," Vol. 2, p. 982. Montpellier, 1993.
33. Delmon, B., and Grange, P., *in* "Catalyst Deactivation 1980" (B. Delmon and G. F. Froment, Eds.), Proc. 2nd Int. Symp. Catal. Deact., p. 363. Elsevier, Amsterdam, 1980.